Knockdown of mesenchymal stem cell-derived exosomal LOC100129516 suppresses the symptoms of atherosclerosis via upregulation of the PPARγ/LXRα/ABCA1 signaling pathway

LIMIN SUN[1,2], XIN HE[3], TAO ZHANG[2], YALING HAN[4] and GUIZHOU TAO[1,3]

[1]Department of Medicine, Soochow University, Suzhou, Jiangsu 215123; Departments of [2]General Practice and [3]Cardiology, The First Affiliated Hospital of Jinzhou Medical University, Jinzhou, Liaoning 121001; [4]Department of Cardiology, General Hospital of Northern Theater Command, Shenyang, Liaoning 110016, P.R. China

Received June 1, 2021; Accepted September 9, 2021

DOI: 10.3892/ijmm.2021.5041

Abstract. Mesenchymal stem cell (MSC) therapy has potential applications in treating atherosclerosis and coronary heart disease (CAD). Previous studies have demonstrated that MSCs are the most preferable sources of therapeutic exosomes, which carry long non-coding RNAs and participate in the progression of atherosclerosis. The results of our previous bioinformatics study demonstrated that the levels of LOC100129516 were significantly upregulated in peripheral blood mononuclear cells obtained from patients with CAD. However, the biological role of LOC100129516 in the development of atherosclerosis remains to be elucidated. In the present study, THP-1 cells were treated with oxidized low-density lipoproteins to induce foam cell formation *in vitro*. Reverse transcription-quantitative PCR (RT-qPCR) was performed to detect the levels of LOC100129516 in THP-1 macrophage-derived foam cells. In addition, an *in vivo* model of atherosclerosis was established using Apolipoprotein E (ApoE) knockout ($ApoE^{-/-}$) mice. The results of the RT-qPCR assays demonstrated that the levels of LOC100129516 were upregulated in THP-1 macrophage-derived foam cells. MSC-derived exosomes were able to deliver small interfering (si)-LOC100129516 to THP-1 cells to reduce the levels of LOC100129516. Moreover, transfection of si-LOC100129516 via exosomal delivery significantly decreased the levels of total cholesterol (TC), free cholesterol and cholesterol ester in THP-1 macrophage-derived foam cells. Exosomal-mediated delivery of si-LOC100129516 decreased TC levels and low-density lipoprotein levels in the $ApoE^{-/-}$ atherosclerosis mouse model. Mechanistically, exosomal-mediated delivery of si-LOC100129516 promoted cholesterol efflux by activating the peroxisome proliferator-activated receptor γ (PPARγ)/liver X receptor α (LXRα)/phospholipid-transporting ATPase ABCA1 (ABCA1) signaling pathway *in vitro* and *in vivo*. Collectively, these results suggested that exosomal-mediated delivery of si-LOC100129516, in which the exosomes were derived from MSCs, promoted cholesterol efflux and suppressed intracellular lipid accumulation, ultimately alleviating the progression of atherosclerosis via stimulation of the PPARγ/LXRα/ABCA1 signaling pathway.

Correspondence to: Dr Guizhou Tao, Department of Medicine, Soochow University, 199 Renai Road, Suzhou, Jiangsu 215123, P.R. China
E-mail: taoguizhou2015@126.com

Key words: atherosclerosis, mesenchymal stem cells, LOC100129516, exosome, peroxisome proliferator-activated receptor γ/liver X receptor α/phospholipid-transporting ATPase ABCA1

Introduction

Atherosclerosis is a chronic inflammatory disease characterized by proliferative lesions in the lining of the arteries, which has a serious impact on the quality of life of patients with the disease (1,2). Atherosclerosis involves arterial wall thickening, sclerosis, loss of elasticity and lumen narrowing (1,2), and is the primary cause of the development of coronary heart disease (CAD) (3). However, the specific cause of atherosclerosis remains to be elucidated (2). Extensive investigations into the etiology of atherosclerosis have demonstrated that it is a multi-etiological disease (4). The collective results of previous studies demonstrated that patients with hyperlipidemia, high blood pressure and diabetes, and patients who smoke experience an increased risk of developing atherosclerosis (5,6). Therapeutic methods that target atherosclerosis can be grouped according to the severity of the disease, including acute, general, drug-based, surgical and Traditional Chinese medicine-based treatments (7-10). Although current strategies for the treatment of atherosclerosis are continuously improving, the mortality rate of atherosclerosis remains high (11). Thus, further investigations into novel therapeutic methods for the treatment of atherosclerosis are required.

Macrophages are common phagocytes found in the blood, lymphatic and mammalian tissue (12), which play important roles in normal development, homeostasis, tissue repair and in the immune response to pathogens (13). Previous studies have reported that macrophages use chemotaxis induced by

inflammatory factors produced during oxidized low-density lipoprotein (ox-LDL) modification, and phagocytosis of ox-LDLs in large quantities induces the formation of foam cells, leading to the development of atherosclerotic lesions (14-16). The functional changes of macrophages are closely associated with the formation and development of atherosclerosis (14-16).

Mesenchymal stem cells (MSCs) are a type of pluripotent stem cell with self-renewal and multidirectional differentiation capacities (17). In addition, MSCs are safe and effective for tissue repair and regeneration in cardiovascular diseases, such as CAD (18). Exosomes are small membrane vesicles (40-100 nm in diameter) that are secreted by a variety of cells, including MSCs (19). Furthermore, exosomes are extensively involved in intercellular communication via transport of proteins, DNA, microRNA (miRNA/miR), long non-coding (lnc)RNA and mRNAs (20). The results of a previous study demonstrated that lncRNAs secreted by MSCs are delivered into recipient cells via exosomes, participating in the progression of CAD (21).

lncRNAs are a class of non-coding RNAs with a length of >200 nucleotides, which are involved in various regulatory processes, such as transcriptional silencing, transcriptional activation, chromosome modification and intra nuclear transport (22,23). It has previously been reported that lncRNAs are closely associated with the occurrence, development, prevention and treatment of CAD (24,25). In our previous study, bioinformatics analysis revealed that LOC100129516 expression was upregulated in peripheral blood mononuclear cells (PBMCs) from patients with CAD, compared with PBMCs from healthy controls (in press). In addition, LOC100129516 knockout exhibited a protective effect on the ox-LDL-induced proliferation inhibition of human umbilical vein endothelial cells (HUVECs).

However, the biological role of MSC-derived exosomal LOC100129516 in atherosclerosis remains to be elucidated. In the present study, MSC-derived exosomal-mediated delivery of small interfering RNA (siRNA/si)-LOC100129516 increased cholesterol excretion and suppressed intracellular lipid accumulation in THP-1 macrophage-derived foam cells and Apolipoprotein E (ApoE) knockout ($ApoE^{-/-}$) mice with atherosclerosis. These results suggested that the exosomal-mediated delivery of si-LOC100129516 alleviated atherosclerosis development both *in vitro* and *in vivo*. Thus, the aim of the present study was to explore novel strategies for atherosclerosis treatment.

Materials and methods

Cell culture and construction of the foam cell model. The human acute monocytic leukemia cell line, THP-1, and human vascular smooth muscle cells were obtained from the American Type Culture Collection. Human bone marrow MSCs were purchased from Procell, Inc. The cells were cultured in RPMI-1640 medium containing 10% FBS and 2 mM glutamine (Sigma Aldrich; Merck KGaA) in a humidified incubator supplied with 5% CO_2 at 37˚C. MSCs and vascular smooth muscle cells were primary cells (commercialized), which have not been immortalized.

To construct the foam cell model, THP-1 cells or vascular smooth muscle cells were exposed to phorbol myristate acetate (100 nM; Sigma-Aldrich; Merck KGaA) for 24 h, and subsequently incubated with 50 μg/ml ox-LDL for 48 h, as described previously (26).

Reverse transcription-quantitative (RT-q)PCR. Total RNA was extracted from cells using TRIzol® reagent (Invitrogen; Thermo Fisher Scientific, Inc.). Subsequently, total RNA was reverse transcribed into cDNA using an EntiLink™ 1st Strand cDNA Synthesis kit according to the manufacturer's protocol (ELK Biotechnology, Co., Ltd.). The temperature and duration of RT were as follows: 37˚C for 60 min and 85˚C for 5 min. qPCR was performed using a SYBR® Premix Ex Taq™ II kit (ELK Biotechnology Co., Ltd.) on a 7900HT system (Applied Biosystems; Thermo Fisher Scientific, Inc.) as follows: 60˚C for 1 min, 90˚C for 15 min, followed by 40 cycles of 90˚C for 15 sec and 55˚C for 60 sec. β-actin was used as an internal control. The standard $2^{-\Delta\Delta Cq}$ method was used for data analysis (27). The following primer sequences were used: β-actin forward, 5'-GTCCACCGCAAATGCTTCTA-3' and reverse, 5'-TGCTGTCACCTTCACCGTTC-3'; and LOC100129516 forward, 5'-GAAAGGGGACTCAGCCATCAT-3' and reverse, 5'-TGCCAAAAACATTAAGTGAGGTG-3'.

Cell transfection. si-LOC100129516 and siRNA-control (ctrl) were purchased from Guangzhou RiboBio Co., Ltd. A total of 10 nM si-LOC100129516 or siRNA-ctrl was transfected into MSCs, THP-1 cells or vascular smooth muscle cells using Lipofectamine® 2000 (Thermo Fisher Scientific, Inc.) for 24 h. The sequences of siRNAs used were as follows: si-LOC100129516, 5'-CCCAGGCTACCATCCCTCCAAATAA-3' and siRNA-ctrl, 5'-CCCATCGTACCTCCCAACCAGATAA-3'.

Isolation and characterization of exosomes. Supernatant from the culture of MSCs was removed and placed into a sterile enzyme-free 15 ml centrifuge tube. The samples were centrifuged at 2,000 x g at 4˚C for 30 min to remove cells and debris. A total of 0.5 ml Total Exosome Isolation reagent (Invitrogen; Thermo Fisher Scientific, Inc.) was added to the samples. Subsequently, the exosome samples were centrifuged at 10,000 x g at 25˚C for 10 min and resuspended with 100 μl 1X PBS. The exosomes were obtained, and a BCA assay (Aspen Biosciences, LLC) was used to detect the corresponding concentration of the exosomes. Transmission electron microscopy (TEM) and Nanoparticle Tracking Analysis (NTA) assays were used to identify the exosomes, as described previously (28). Western blot analysis was used to detect the expression levels of exosomal-specific surface biomarkers, CD63 and tumor susceptibility gene 101 (TSG101).

Exosome labeling and uptake. THP-1 cells were treated with MSC-derived exosomes at 37˚C for 24 h. Subsequently, cells were labeled for 24 h at 4˚C with PKH26 red membrane dye (1:1,000; Biolab Co., Ltd.; cat. no. HR9070). In addition, fluorescent phalloidin dye (Thermo Fisher Scientific, Inc.) was used to label the cytoskeleton overnight at 4˚C, and DAPI was used to stain the nuclei at room temperature for 10 min. Images were captured using a fluorescence microscope (magnification, x200; Olympus Corporation).

Western blot analysis. Proteins were isolated using protein lysis buffer (Beyotime Institute of Biotechnology) and quantified using a BCA protein assay kit. A total of 30 μg protein per lane was loaded on a 10% SDS gel, resolved using SDS-PAGE and transferred to a PVDF membrane. The membrane was subsequently incubated with the following primary antibodies: Anti-CD63 (1:1,000; cat. no. ab134045; Abcam), anti-TSG101 (1:1,000; cat. no. ab125011; Abcam), anti-CD9 (1:1,000; cat. no. ab236630; Abcam) anti-cleaved ccaspase-3 (1:1,000; cat. no. ab32042; Abcam), anti-peroxisome proliferator-activated receptor γ (PPARγ; 1:1,000; cat. no. ab178860; Abcam), anti-liver X receptor α (LXRα; 1:1,000; cat. no. ab176323; Abcam), anti-phospholipid-transporting ATPase ABCA1 (ABCA1; 1:1,000; cat. no. ab66217; Abcam) and β-actin (1:1,000; cat. no. ab8226; Abcam) at 4˚C overnight. Following the primary antibody incubation, membranes were incubated with HRP-conjugated goat anti-rabbit IgG secondary antibody (1:5,000; cat. no. ab7090; Abcam) at room temperature for 1 h. Subsequently, the protein bands were detected using an ECL kit (Thermo Fisher Scientific, Inc.).

ELISA. The levels of total cholesterol (TC), free cholesterol (FC) and cholesterol ester (CE) in THP-1 macrophage-derived foam cells were measured using ELISA. The levels of TC and low-density lipoprotein cholesterol (LDL-C) were also measured in the plasma of mice using ELISA kits, according to the manufacturer's protocol. The TC assay kit (cat. no. A111-1-1) and LDL-C assay kit (cat. no. A113-1-1) were obtained from Nanjing Jiancheng Bioengineering Institute. A Micro FC Content assay kit (cat. no. BC1895) was purchased from Beijing Solarbio Science & Technology Co., Ltd. The CE content was calculated using the following equation: CE = TC content - FC content.

Observation of adipocytes. Oil red O staining was used to observe the distribution of adipose cells in THP-1 macrophage-derived foam cells. Oil red O was obtained from Beijing Solarbio Science & Technology Co., Ltd. Cells were stained with Oil red O for 5 min at room temperature. The images were observed under a fluorescence microscope.

Flow cytometry assay. THP-1 cells were trypsinized and resuspended in binding buffer. Then, cells were stained with 5 μl Annexin V-FITC (BD Biosciences) and propidium iodide (PI; BD Biosciences) in the dark at 37˚C for 30 min. Flow cytometry (FACScan™; BD Biosciences) was applied to analyze the apoptosis rate using CellQuest™ software version 5.1 (BD Biosciences).

Nitrobenzoxadiazole-labeled cholesterol efflux assay. THP-1 macrophage-derived foam cells were incubated with 1 μg/ml NBD-cholesterol in RPMI-1640 medium containing 0.2% BSA for 24 h. A total of 15 μg/ml Apolipoprotein A1 (ApoA1; Sigma-Aldrich; Merck KGaA) or 50 μg/ml high-density lipoprotein (HDL) was used to induce cholesterol efflux. A microplate reader (Tecan Infinite M200) was used to measure NBD-cholesterol efflux (515 nm).

In vivo model of atherosclerosis. Male ApoE$^{-/-}$ mice (n=24, age, 8 weeks; weight, 20-25 g) were purchased from the Beijing Vital River Laboratory Animal Technology Co., Ltd. Animals were housed in a specific pathogen-free animal facility with 60% humidity at a constant temperature of 24±2˚C. To establish the *in vivo* atherosclerosis model, animals were randomly divided into four groups: i) Control group, containing ApoE$^{-/-}$ mice fed on a standard 4% fat diet (cat. no. D12450B; Beijing HFK Bioscience; ii) atherosclerosis (AS) group, containing ApoE$^{-/-}$ mice fed on a high-fat diet with 60% of total calories derived from fat (cat. no. D12492; Beijing HFK Bioscience) and an intravenous injection of 200 μl PBS per dose; iii) siRNA-ctrl exosome (Exo) + AS; and iv) si-LOC100129516 Exo + AS groups, containing ApoE$^{-/-}$ mice fed on a high-fat diet, with an injection of siRNA-ctrl Exo or si-LOC100129516 Exo via the tail vein twice a week. All mice were sacrificed using CO_2 (30% volume/min) and blood samples and arteries were collected for subsequent experiments. All animal procedures were approved by The Committee of the First Affiliated Hospital of Jinzhou Medical University (approval no. FAHJMU20210113). The National Institute of Health Guide for the Care and Use of Laboratory Animals was strictly followed (29).

Oil red O and hematoxylin and eosin (H&E) staining of arteries. The arteries of the mice were perfused with PBS and separated. The arteries of mice were subsequently stained with Oil red O and H&E as described previously (30).

Statistical analysis. All results are presented as the mean ± standard deviation. Data were analyzed using a one-way ANOVA followed by a Tukey's post hoc test, using GraphPad Prism software (version 7.0; GraphPad Software, Inc.). $P<0.05$ was considered to indicate a statistically significant difference.

Results

LOC100129516 is upregulated in THP-1 macrophage-derived foam cells. In our previous study, results of bioinformatics analysis demonstrated that the levels of LOC100129516 were upregulated in PBMCs obtained from patients with CAD. In order to identify the expression levels and role of LOC100129516 in atherosclerosis, the levels of LOC100129516 were determined. As shown in Fig. 1, the expression of LOC100129516 in THP-1 macrophage-derived foam cells was significantly higher compared with the expression levels in THP-1 macrophages.

si-LOC100129516 is transferred from MSCs to THP-1 macrophages via exosomes. MSC-based therapy has emerged as a cell-based therapy for treating atherosclerosis (31). The results of a previous study demonstrated that exosomes carrying non-coding RNAs are involved in cell-cell communication between MSCs and macrophages (18). The present study aimed to investigate whether si-LOC100129516 could be transferred from MSCs to THP-1 macrophages via exosomes. As shown in Fig. 2A, transfection of si-LOC100129516 notably decreased the levels of LOC100129516 in MSCs, compared with the siRNA-ctrl group. Furthermore, exosomes were isolated from the culture supernatant of MSCs (MSCs-Exo), and MSCs were transfected with siRNA-ctrl (siRNA-ctrl/MSCs-Exo)

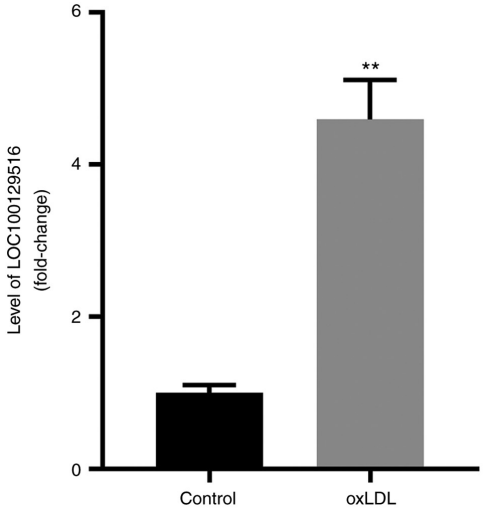


Figure 1. LOC100129516 expression is upregulated in THP-1 macrophage-derived foam cells. THP-1 macrophages were treated with 50 μg/ml ox-LDL for 48 h to construct a foam cell model, and the mRNA levels of LOC100129516 in THP-1 macrophage cells and THP-1 macrophage-derived foam cells were determined. n=3. **P<0.01 vs. control group. ox-LDL, oxidized low density lipoproteins.

or si-LOC100129516 (si-LOC100129516/MSCs-Exo). TEM and NTA results indicated that MSC-derived exosomes were round, phospholipid bilayer-enclosed structures with a diameter of 40-100 nm (Fig. 2B and C). Moreover, markers of exosomes, such as CD9, CD63 and TSG101 were detected using western blot analysis (Fig. 2D). The levels of LOC100129516 were significantly decreased in si-LOC100129516/MSCs-Exo compared with that in siRNA-ctrl/MSCs-Exo (Fig. 2E). To investigate whether MSC-derived exosomes and MSC-derived exosomes transfected with si-LOC100129516 were internalized by THP-1 macrophages, exosomes were labeled with PKH26 dye and incubated with THP-1 macrophages. As demonstrated in Fig. 2F, MSC-derived exosomes were absorbed by THP-1 macrophages. Furthermore, si-LOC100129516/MSCs-Exo significantly decreased the levels of LOC100129516 in THP-1 macrophages (Fig. 2G). Collectively, these results indicated that si-LOC100129516 can be transferred from MSCs to THP-1 macrophages via exosomes.

Exosomal-mediated delivery of si-LOC100129516 inhibits apoptosis in THP-1 macrophage-derived foam cells. To investigate whether exosomal-mediated delivery of si-LOC100129516 affected the apoptosis in THP-1 macrophage-derived foam cells, flow cytometry was performed. As shown in Fig. 3A, ox-LDL significantly induced apoptosis in THP-1 macrophages compared with the control group. However, these changes were partially reversed by si-LOC100129516/MSCs-Exo. In addition, si-LOC100129516/MSCs-Exo significantly downregulated the expression of cleaved ccaspase-3 in THP-1 macrophage-derived foam cells (Fig. 3B and C). Silencing of LOC100129516 or si-LOC100129516/MSCs-Exo notably restored ox-LDL-induced increase of vascular smooth muscle cell viability (Fig. S1A), and LOC100129516 knockdown did not affect the apoptosis of THP-1 cells (Fig. S1B). These results indicated that exosomal-mediated delivery of si-LOC100129516 inhibited the apoptosis of THP-1 macrophage-derived foam cells.

Exosomal-mediated delivery of si-LOC100129516 inhibits lipid accumulation in THP-1 macrophage-derived foam cells. The role of exosomal-mediated delivery of si-LOC100129516 in lipid accumulation in THP-1 macrophage-derived foam cells was investigated. As indicated in Fig. 4A-C, ox-LDL markedly increased the levels of TC, FC and CE in THP-1 macrophages compared with the control group. However, these ox-LDL-induced changes were reversed by si-LOC100129516/MSCs-Exo. In addition, the Oil-Red O staining results indicated that ox-LDL significantly increased intracellular lipid accumulation compared with the control group. However, this phenomenon was also reversed in the presence of si-LOC100129516/MSCs-Exo (Fig. 4D). Collectively, these results demonstrated that exosomal-mediated delivery of si-LOC100129516 inhibited the lipid accumulation in THP-1 macrophage-derived foam cells.

Exosomal-mediated delivery of si-LOC100129516 increases cholesterol efflux in THP-1 macrophage-derived foam cells via upregulation of the PPARγ/LXRα/ABCA1 signaling pathway. Reverse cholesterol transport (RCT) is a key process in removing excessive cholesterol from cells (32). HDL and ApoA1 proteins serve important roles in the RCT pathway, contributing to the efflux of excess cellular cholesterol (33-35). Thus, the effect of exosomal-mediated delivery of si-LOC100129516 on cholesterol efflux was examined in the present study. As shown in Fig. 5A and B, si-LOC100129516/MSCs-Exo markedly promoted cholesterol efflux to HDL and ApoA1. In addition, the PPARγ/LXRα/ABCA1 signaling pathway plays an important role in atherosclerosis progression via promotion of cholesterol efflux, maintenance of cholesterol balance and inhibition of foam cell formation (36,37). Thus, the protein levels of PPARγ, LXRα and ABCA1 in THP-1 macrophage-derived foam cells were detected using western blot analysis. As indicated in Fig. 5C-F, ox-LDL significantly decreased the expression levels of PPARγ, LXRα and ABCA1 in THP-1 macrophages, compared with the control group. However, these changes were partially reversed by si-LOC100129516/MSCs-Exo. Thus, exosomal-mediated delivery of si-LOC100129516 increased cholesterol efflux in THP-1 macrophage-derived foam cells via increasing the activity of the PPARγ/LXRα/ABCA1 signaling pathway.

Exosomal-mediated delivery of si-LOC100129516 suppresses atherosclerosis progression in vivo via upregulation of the PPARγ/LXRα/ABCA1 signaling pathway. To further explore the role of exosomal-mediated delivery of si-LOC100129516 on the progression in atherosclerosis, a mouse model of atherosclerosis was established. As demonstrated in Fig. 6A, the expression levels of LOC100129516 was significantly upregulated in aortic tissues in the atherosclerotic mouse model. However, this phenomenon was reversed by si-LOC100129516/MSCs-Exo treatment. In addition, mice that were fed a high-fat diet demonstrated a distinct thickening of the blood vessel wall and notable plaque formation in the aortic tissue. However, this effect was reversed by si-LOC100129516/MSCs-Exo treatment (Fig. 6B). Moreover, the results of the Oil red O staining assay revealed lipid accumulation and atherosclerotic plaque formation in the aortic tissue of the atherosclerotic mice compared with the control group, and this was reversed

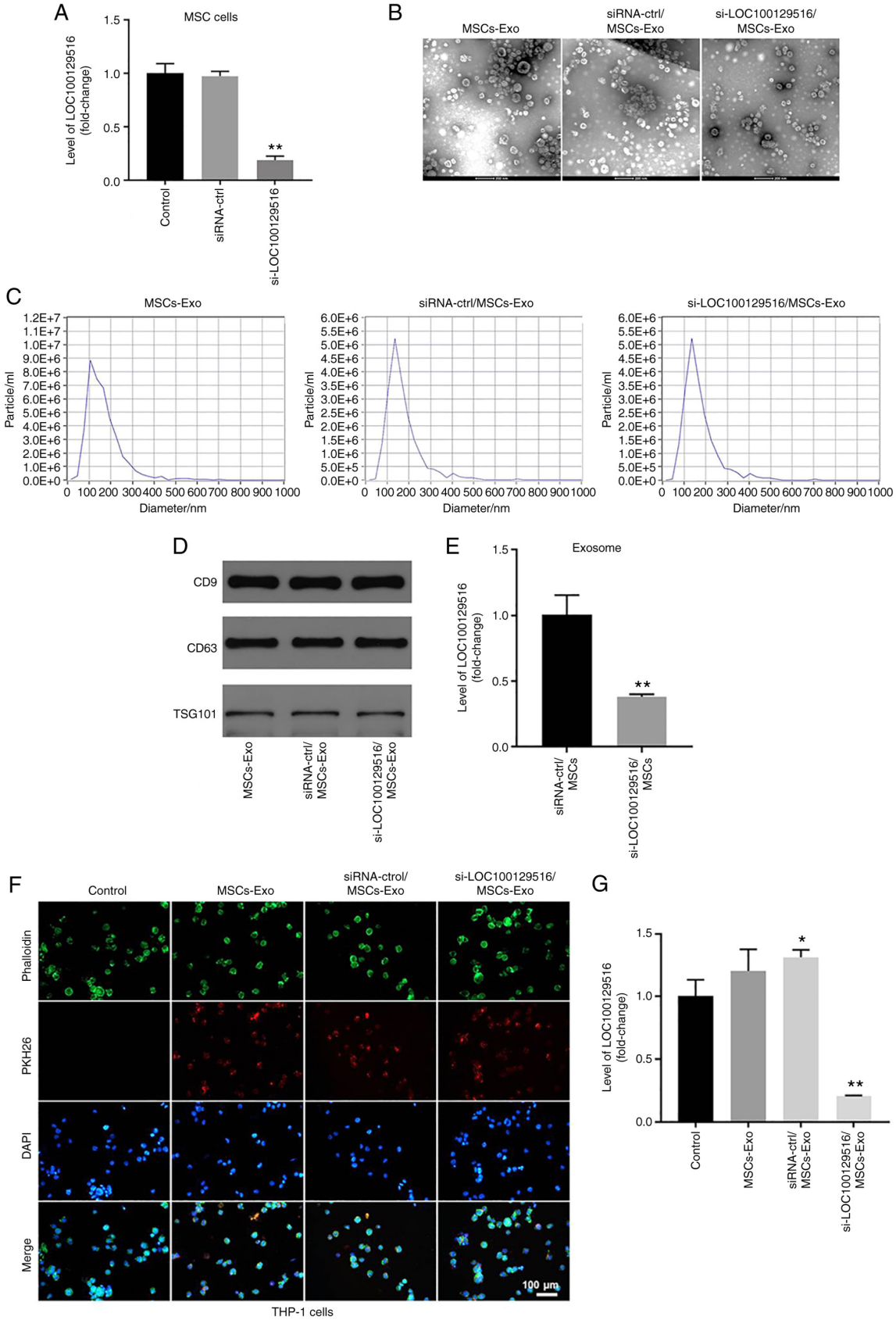


Figure 2. si-LOC100129516 can be transferred from MSCs to THP-1 macrophages via exosomes. (A) RT-qPCR was used to detect the levels of LOC100129516 in MSCs transfected with si-LOC100129516 or siRNA-ctrl. (B and C) Exosomes were isolated from MSCs that were transfected with si-LOC100129516 or siRNA-ctrl. Transmission electron microscopy (magnification, 200x) and Nanoparticle Tracking Analysis assays were used to identify exosomes. (D) Western blotting was used to detect expression of exosomal surface markers CD9, CD63 and TSG101. (E) RT-qPCR was used to detect the level of LOC100129516 in exosomes. (F) The MSC-derived exosomes absorbed by THP-1 macrophages were observed under a fluorescence microscope (magnification, 200x). Red color, exosome; green color, SHG44 cells; blue color, cell nucleus. Scale bar, 100 μm. (G) RT-qPCR was used to detect the levels of LOC100129516 in THP-1 macrophages after incubation with the indicated exosomes. n=3. *P<0.05, **P<0.01 vs. control group. siRNA, small interfering RNA; MSC, mesenchymal stem cell; RT-qPCR, reverse transcription-quantitative PCR; ctrl, control; TSG101, tumor susceptibility gene 101; Exo, exosome.

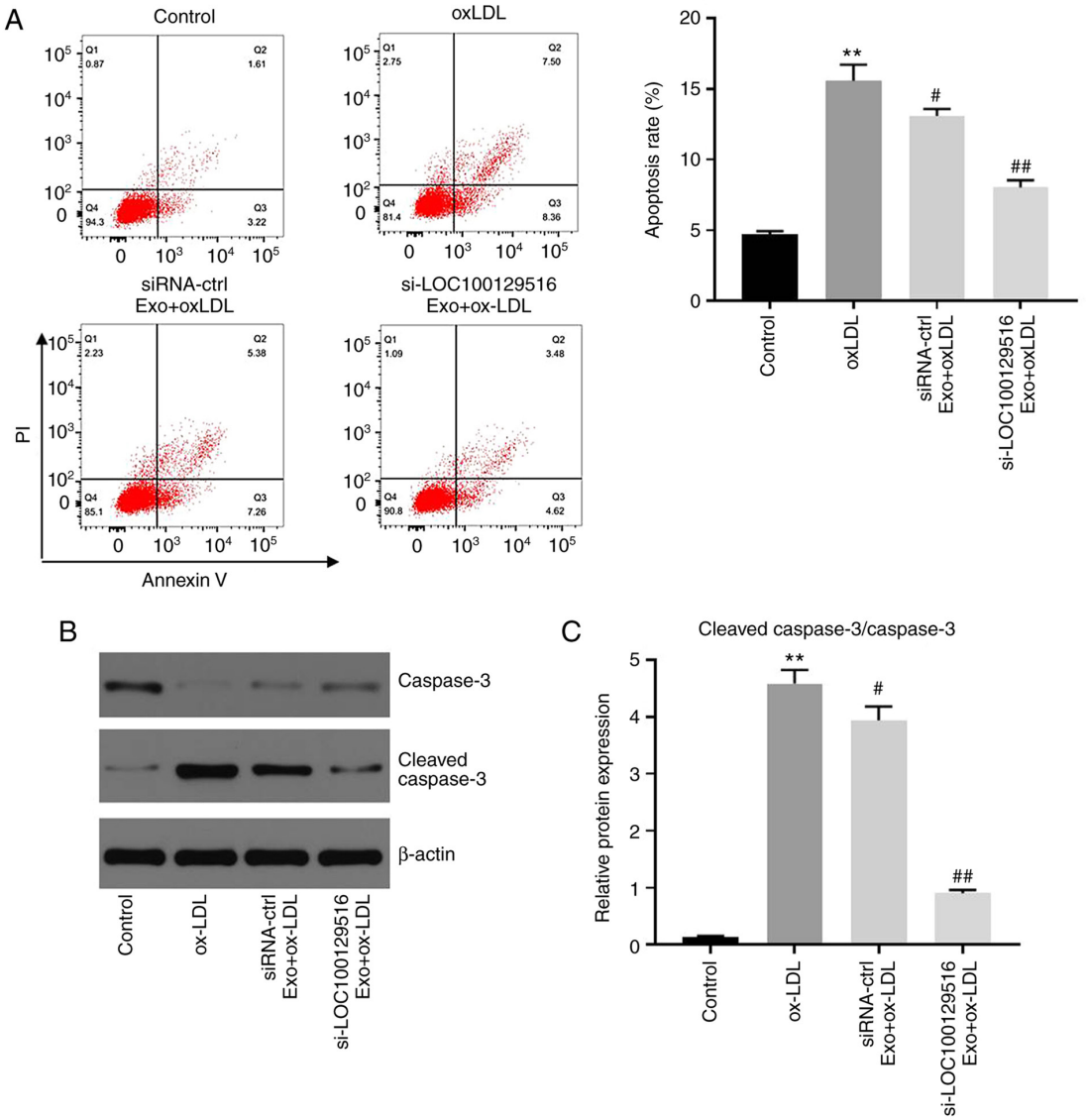


Figure 3. Exosomal si-LOC100129516 inhibits the apoptosis in THP-1 macrophage-derived foam cells. MSCs were transfected with si-LOC100129516 or siRNA-ctrl. In addition, ox-LDL-treated THP-1 macrophages were incubated with exosomes derived from transfected MSCs. (A) Flow cytometry analysis was used to analyze cell apoptosis. (B and C) Western blotting was used to detect the expression levels of total caspase-3 and cleaved ccaspase-3 in cells. n=3. **P<0.01 vs. control group; $^{\#}$P<0.01, $^{\#\#}$P<0.01 vs. ox-LDL group. siRNA, small interfering RNA; MSC, mesenchymal stem cell; ox-LDL, oxidized low density lipoproteins; Exo, exosome.

by si-LOC100129516/MSCs-Exo treatment (Fig. 6B). si-LOC100129516/MSCs-Exo markedly reduced the plasma levels of TC and LDL-C in ApoE$^{-/-}$ mice with atherosclerosis (Fig. 6C). Furthermore, si-LOC100129516/MSCs-Exo significantly upregulated the expression levels of PPARγ, LXRα and ABCA1 in the aortic tissues of ApoE$^{-/-}$ mice with atherosclerosis (Fig. 7A-D). Collectively, these results indicated that exosomal-mediated delivery of si-LOC100129516 suppressed atherosclerosis progression *in vivo* via upregulation of the PPARγ/LXRα/ABCA1 signaling pathway.

Discussion

MSCs have been demonstrated to be effective for the treatment of atherosclerosis, due to their ability to repair tissue, in addition to their anti-inflammatory and immunological properties (38). MSCs can be isolated from several types of tissues, including bone marrow, the umbilical cord, placenta, adipose tissue and human gingiva (39,40). MSCs that are used for the treatment of atherosclerotic plaques are primarily derived from the bone marrow (39), but can also be obtained the gingiva (41). In addition, MSC-derived exosomes have been a key focus of research for several decades (42). Exosomes are macrovesicles 30-150 nm in size that are secreted by MSCs via a paracrine mechanism (43). Exosomes derived from MSCs carry a number of bioactive substances, such as proteins, miRNAs and lncRNAs, and play an important role in the treatment of cardiovascular diseases, such as atherosclerosis (18,43,44). A high expression level of lncRNA-Ang362 was shown to lead to a poor prognosis in patients with CAD (45). Moreover, Mao *et al* (46) demonstrated that MSC-derived exosomal lncRNA Krüppel-like factor 3 antisense RNA 1 alleviated the development of myocardial infarction via the miR-138-5p/Sirtuin-1 axis (46). However, the functions of a

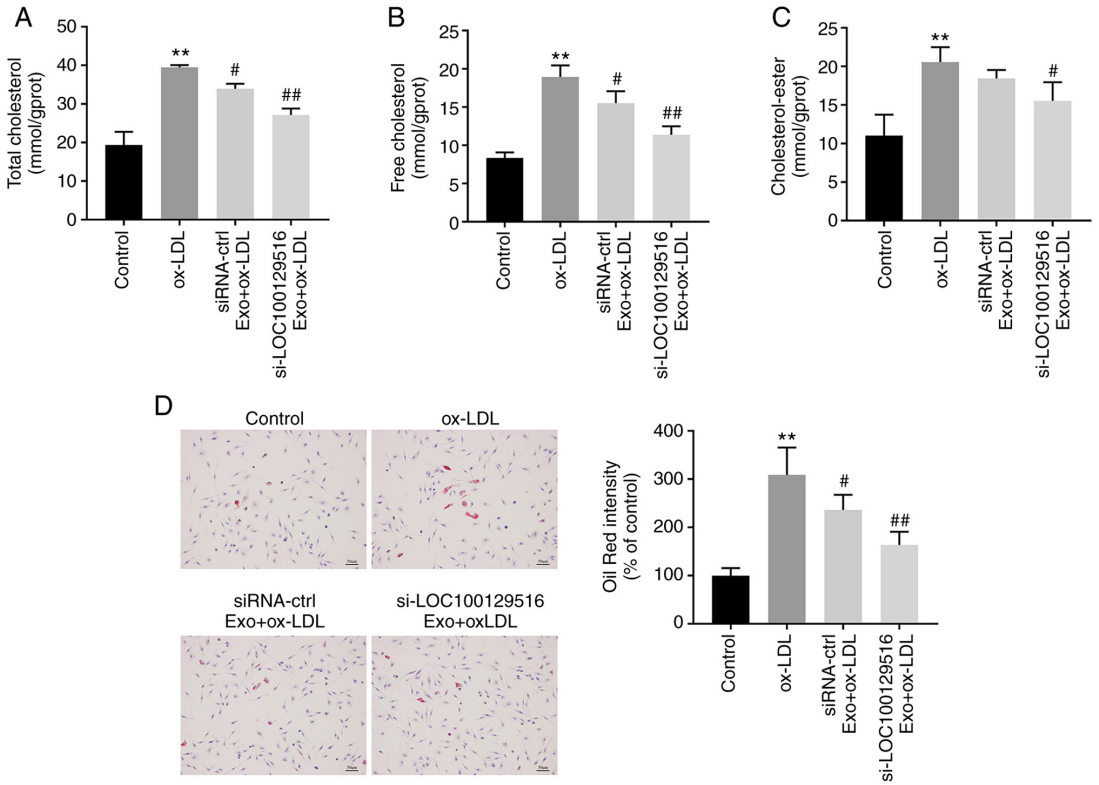


Figure 4. Exosomal si-LOC100129516 inhibits lipid accumulation in THP-1 macrophage-derived foam cells. MSCs were transfected with si-LOC100129516 or siRNA-ctrl. In addition, ox-LDL-treated THP-1 macrophages were incubated with exosomes derived from transfected MSCs. (A-C) The levels of TC, FC and CE in cells were measured by ELISA. (D) Oil red O staining assay was used to observe intracellular lipid accumulation. n=3. **P<0.01 vs. control group; $^{\#}$P<0.01, $^{\#\#}$P<0.01 vs. ox-LDL group. siRNA, small interfering RNA; MSC, mesenchymal stem cell; ox-LDL, oxidized low density lipoproteins; ctrl, control; Exo, exosome.

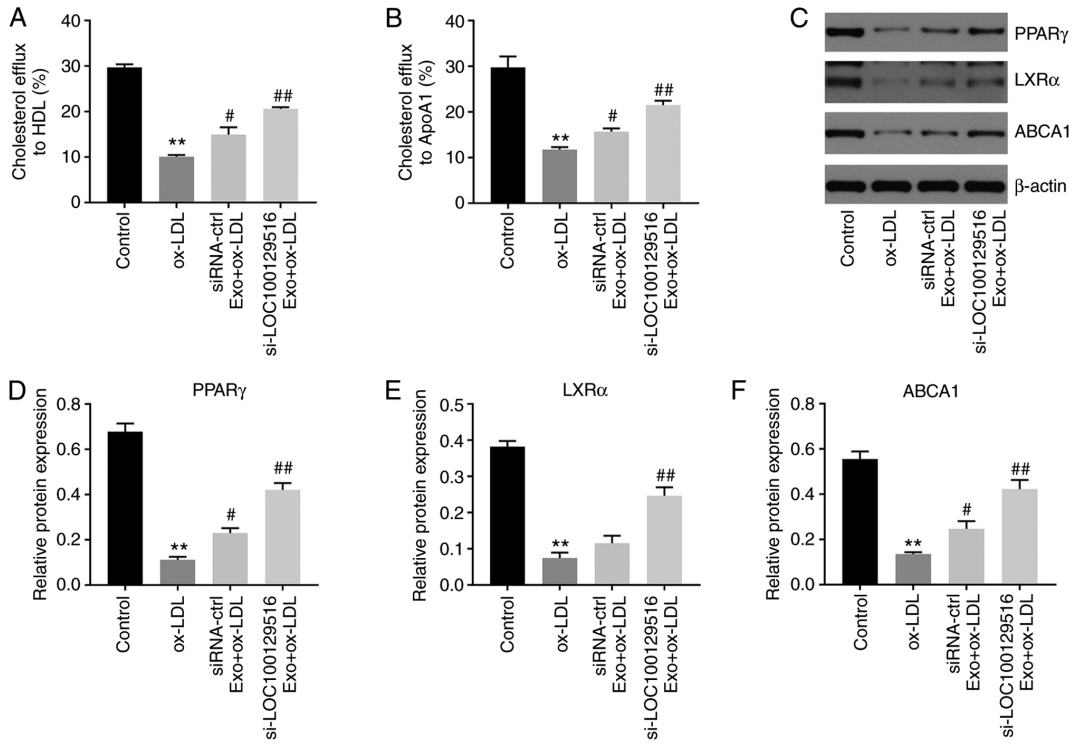


Figure 5. Exosomal si-LOC100129516 increases cholesterol excretion in THP-1 macrophage-derived foam cells by increasing the activity of the PPARγ/LXRα/ABCA1 signaling pathway. MSCs were transfected with si-LOC100129516 or siRNA-ctrl. In addition, ox-LDL-treated THP-1 macrophages were incubated with exosomes derived from transfected MSCs. (A and B) Quantification of cholesterol efflux to high-density lipoprotein cholesterol and ApoA1 in cells. (C-F) Western blot assay was used to detect the expression levels of PPARγ, LXRα and ABCA1 in cells. n=3. **P<0.01 vs. control group; $^{\#}$P<0.01, $^{\#\#}$P<0.01 vs. ox-LDL group. siRNA, small interfering RNA; MSC, mesenchymal stem cell; ox-LDL, oxidized low density lipoproteins; ctrl, control; PPARγ, peroxisome proliferator-activated receptor γ; LXRα, liver X receptor α; ABCA1, phospholipid-transporting ATPase ABCA1; APOA1, apolipoprotein A1; Exo, exosome.

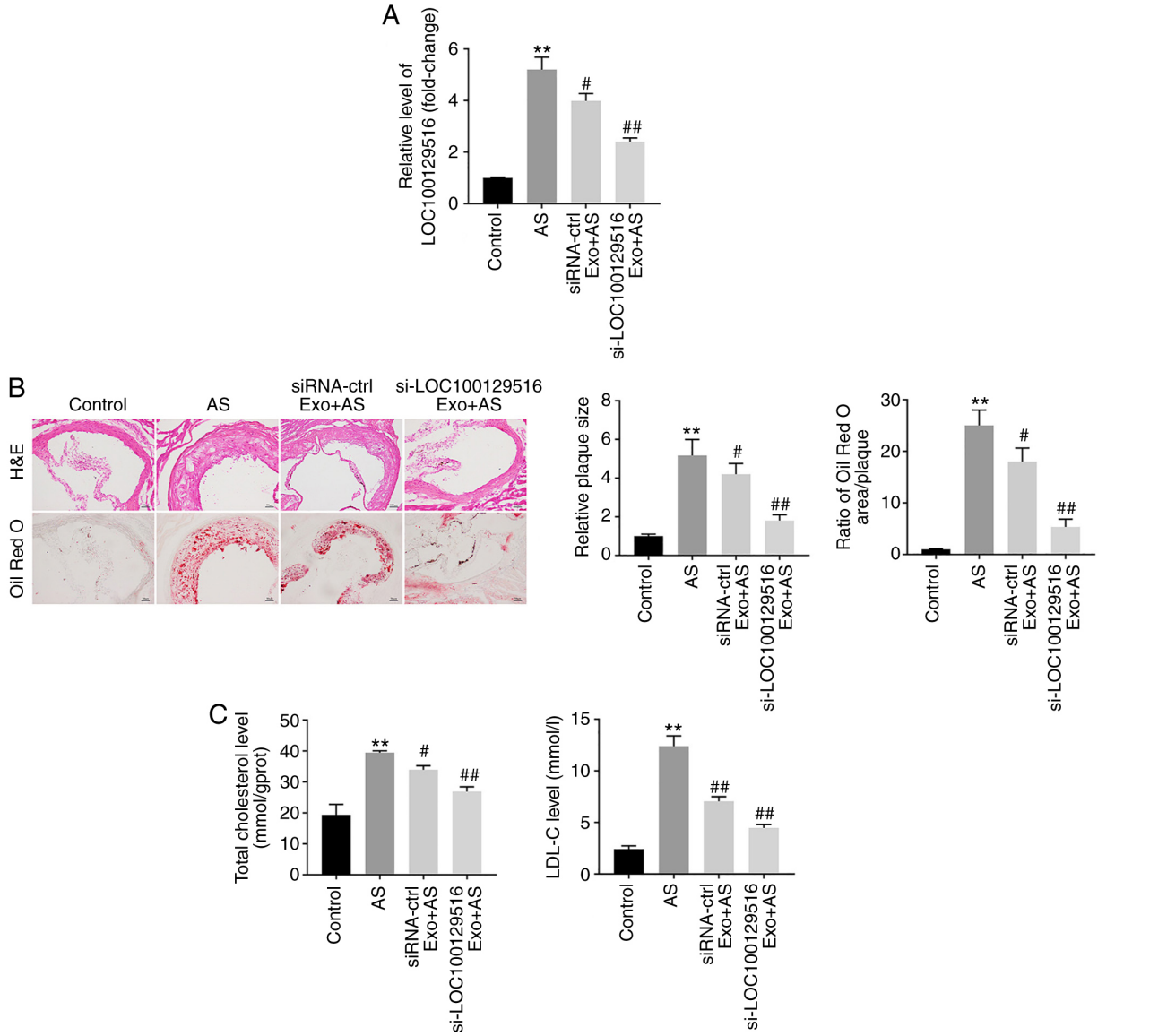


Figure 6. Exosomal si-LOC100129516 suppresses atherosclerotic progression *in vivo*. (A) Reverse transcription-quantitative PCR was used to detect the levels of LOC100129516 in the aortic tissues of ApoE$^{-/-}$ mice. (B) Hematoxylin and eosin staining as well as Oil-red O staining were used to observe aortic plaque formation in the ApoE$^{-/-}$ mice. (C) ELISA kits were used to measure the levels of TC and LDL-C in the plasma of ApoE$^{-/-}$ mice. n=6. **P<0.01 vs. control group; $^{\#}$P<0.01, $^{\#\#}$P<0.01 vs. AS group. siRNA, small interfering RNA; H&E, hematoxylin and eosin; TC, total cholesterol; LDL-C, low-density lipoprotein cholesterol; ctrl, control; AS, atherosclerosis; Exo, exosome.

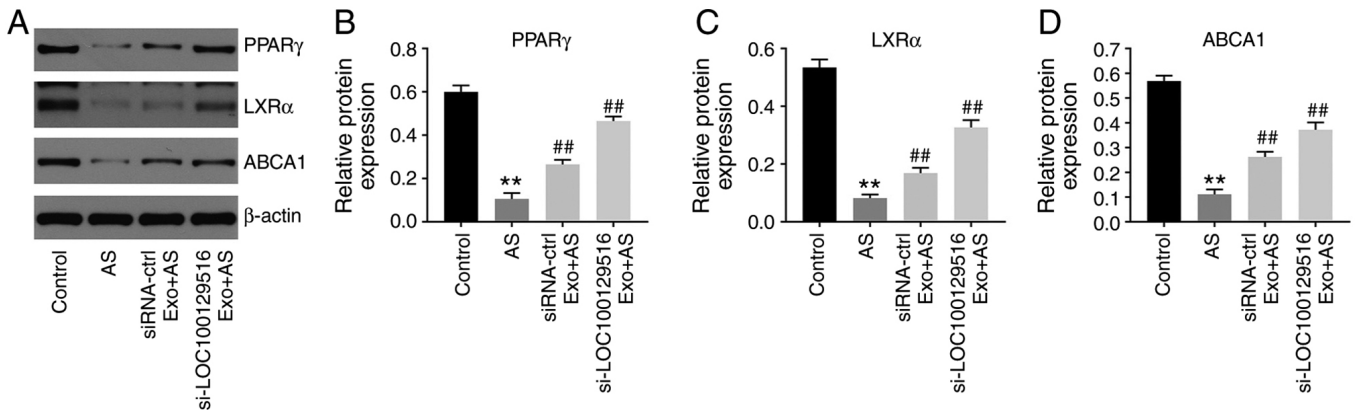


Figure 7. Exosomal si-LOC100129516 suppresses atherosclerotic progression *in vivo* via upregulation of the PPARγ/LXRα/ABCA1 signaling pathway. (A-D) Western blot assays were performed to detect the expression levels of PPARγ, LXRα and ABCA1 in the aortic tissues of ApoE$^{-/-}$ mice. n=6. **P<0.01 vs. control group; $^{\#\#}$P<0.01 vs. AS group. siRNA, small interfering RNA; PPARγ, peroxisome proliferator-activated receptor γ; LXRα, liver X receptor α; ABCA1, phospholipid-transporting ATPase ABCA1; ctrl, control; AS, atherosclerosis; Exo, exosome.

number of lncRNAs in atherosclerosis remain to be elucidated. Thus, it is necessary to identify novel therapeutic targets for the prevention of progression of atherosclerosis. In the present study, it was shown that exosomal LOC100129516 derived from MSCs could suppress ox-LDL-induced HUVEC growth inhibition. Thus, the present study was the first to explore the function of exosomal LOC100129516 in atherosclerosis, suggesting a novel target for the treatment of atherosclerosis.

Li *et al* (47) reported that the overexpression of cyclin-dependent kinase inhibitor 2B antisense RNA 1 reduced lipid accumulation and increased cholesterol efflux in THP-1 macrophage-derived foam cells and in atherosclerotic plaque tissues (47). Moreover, Meng *et al* (48) found that downregulation of lncRNA growth arrest specific 5 reduced lipid accumulation in THP-1 macrophage-derived foam cells, thus inhibiting the progression of atherosclerosis. In the present study, MSC-derived exosomal-mediated delivery of si-LOC100129516 significantly inhibited the apoptosis, intracellular cholesterol accumulation and lipid accumulation of THP-1 macrophage-derived foam cells, consistent with Meng *et al* (48). In the study by Meng *et al* (48), GAS5 knockdown reduced EZH2-mediated transcriptional inhibition of ABCA1 via histone methylation, and ABCA1 served a vital role in atherosclerotic progression (49). Consistently, ABCA1 was found to be regulated by exosomes with downregulated levels of LOC100129516. Therefore, the similar functions between GAS5 and exosomes with downregulated LOC100129516 expression may result in this similarity. Moreover, exosomal-mediated delivery of si-LOC100129516 reduced lipid accumulation and atherosclerotic plaque formation in $ApoE^{-/-}$ mice with atherosclerosis. The results of the present study suggested that exosomal-mediated delivery of si-LOC100129516 inhibited atherosclerosis progression both *in vitro* and *in vivo*. Meanwhile, the present study found that exosomal-mediated delivery of si-NC could also reverse ox-LDL-induced HUVEC growth inhibition. This phenomenon may result from the fact that exosomes have a targeting effect, which can escape the phagocytosis of macrophages (50), highlighting a potential advantage of exosomes as a mode of treatment/delivery *in vivo*.

PPARγ is an effective cholesterol sensor and plays a major role in the treatment of atherosclerosis (51). In addition, PPARγ enhances cholesterol efflux by inducing LXRα and ABCA1 transcription (52). The results of a previous study demonstrated that downregulation of the PPARγ/LXRα/ABCA1 signaling pathway aggravated the progression of atherosclerosis (53). Zhao *et al* (51) revealed that miR-613 inhibited the efflux of cholesterol from THP-1 macrophage-derived foam cells by downregulating the activity of the PPARγ/LXRα/ABCA1 signaling pathway (51). Furthermore, Wang *et al* (54) demonstrated that chrysin enhanced the efflux of cholesterol by regulating the PPARγ/LXRα/ABCA1/ATP binding cassette subfamily G member 1 signaling pathway (54). The results of the present study revealed that si-LOC100129516/MSCs-Exo increased cholesterol excretion by upregulating the PPARγ/LXRα/ABCA1 signaling pathway in THP-1 macrophage-derived foam cells *in vitro*, and in $ApoE^{-/-}$ mice with atherosclerosis *in vivo*.

The present study has some limitations as follows: i) The advantages and disadvantages of exosomal si-LOC100129516 in comparison to treatment with si-LOC100129516 transfection remain unclear; and ii) more in-depth analysis of the signaling pathways regulated by exosomal LOC100129516 in ox-LDL-treated HUVECs is required. In conclusion, MSC-derived exosomal-mediated delivery of si-LOC100129516 promoted cholesterol efflux and suppressed intracellular lipid accumulation, thus alleviating the progression of atherosclerosis by stimulating the PPARγ/LXRα/ABCA1 signaling pathway. The results of the present study highlighted that LOC10012951 may act as a potential target for novel therapeutic strategies in the treatment of atherosclerosis.

Acknowledgements

Not applicable.

Funding

This trial is a physician-initiated study and is supported by a research fund from the Chinese National Key R&D project (contract IDs: 2016YFC1301303 and 2016YFC1301300).

Availability of data and materials

The datasets used and/or analyzed during the present study are available from the corresponding author on reasonable request.

Authors' contributions

LS made major contributions to the conception and design of the study, as well as the drafting of the manuscript. XH and TZ were responsible for data acquisition, data analysis, data interpretation and manuscript revision. GT and YH made substantial contributions to conception and design of the study, and revised the manuscript critically for important intellectual content. All authors have read and approved the final manuscript. YH and LS confirmed the authenticity of all the raw data.

Ethics approval and consent to participate

All animal procedures were approved by the Committee of the First Affiliated Hospital of Jinzhou Medical University (approval no. FAHJMU20210113). The National Institute of Health Guide for the Care and Use of Laboratory Animals was strictly followed.

Patient consent for publication

Not applicable.

Competing interests

The authors declare that they have no competing interests.

References

1. Falk E: Pathogenesis of atherosclerosis. J Am Coll Cardiol 47: C7-C12, 2006.
2. Tedgui A and Mallat Z: Cytokines in atherosclerosis: Pathogenic and regulatory pathways. Physiol Rev 86: 515-581, 2006.

3. Weber C and Noels H: Atherosclerosis: Current pathogenesis and therapeutic options. Nat Med 17: 1410-1422, 2011.
4. Lechner K, von Schacky C, McKenzie AL, Worm N, Nixdorff U, Lechner B, Kränkel N, Halle M, Krauss RM and Scherr J: Lifestyle factors and high-risk atherosclerosis: Pathways and mechanisms beyond traditional risk factors. Eur J Prev Cardiol 27: 394-406, 2020.
5. Shoeibi S: Diagnostic and theranostic microRNAs in the pathogenesis of atherosclerosis. Acta Physiol (Oxf) 228: e13353, 2020.
6. Kunitomo M: Oxidative stress and atherosclerosis. Yakugaku Zasshi 127: 1997-2014, 2007 (In Japanese).
7. Li TT, Wang ZB, Li Y, Cao F, Yang BY and Kuang HX: The mechanisms of traditional Chinese medicine underlying the prevention and treatment of atherosclerosis. Chin J Nat Med 17: 401-412, 2019.
8. Zarzycka B, Nicolaes GA and Lutgens E: Targeting the adaptive immune system: New strategies in the treatment of atherosclerosis. Expert Rev Clin Pharmacol 8: 297-313, 2015.
9. Wang C, Niimi M, Watanabe T, Wang Y, Liang J and Fan J: Treatment of atherosclerosis by traditional Chinese medicine: Questions and quandaries. Atherosclerosis 277: 136-144, 2018.
10. Vaidyanathan K and Gopalakrishnan S: Nanomedicine in the diagnosis and treatment of atherosclerosis - a systematic review. Cardiovasc Hematol Disord Drug Targets 17: 119-131, 2017.
11. Fasolo F, Di Gregoli K, Maegdefessel L and Johnson JL: Non-coding RNAs in cardiovascular cell biology and atherosclerosis. Cardiovasc Res 115: 1732-1756, 2019.
12. Varol C, Mildner A and Jung S: Macrophages: Development and tissue specialization. Annu Rev Immunol 33: 643-675, 2015.
13. Smigiel KS and Parks WC: Macrophages, wound healing, and fibrosis: Recent insights. Curr Rheumatol Rep 20: 17, 2018.
14. Kuznetsova T, Prange KHM, Glass CK and de Winther MPJ: Transcriptional and epigenetic regulation of macrophages in atherosclerosis. Nat Rev Cardiol 17: 216-228, 2020.
15. Moore KJ and Tabas I: Macrophages in the pathogenesis of atherosclerosis. Cell 145: 341-355, 2011.
16. Barrett TJ: Macrophages in atherosclerosis regression. Arterioscler Thromb Vasc Biol 40: 20-33, 2020.
17. Uccelli A, Moretta L and Pistoia V: Mesenchymal stem cells in health and disease. Nat Rev Immunol 8: 726-736, 2008.
18. Li J, Xue H, Li T, Chu X, Xin D, Xiong Y, Qiu W, Gao X, Qian M, Xu J, *et al*: Exosomes derived from mesenchymal stem cells attenuate the progression of atherosclerosis in $ApoE^{-/-}$ mice via miR-let7 mediated infiltration and polarization of M2 macrophage. Biochem Biophys Res Commun 510: 565-572, 2019.
19. Kalluri R and LeBleu VS: The biology, function, and biomedical applications of exosomes. Science 367: eaau6977, 2020.
20. Sasaki R, Kanda T, Yokosuka O, Kato N, Matsuoka S and Moriyama M: Exosomes and hepatocellular carcinoma: From BENCH TO BEDside. Int J Mol Sci 20: 1406 2019.
21. Huang P, Wang L, Li Q, Tian X, Xu J, Xu J, Xiong Y, Chen G, Qian H, Jin C, *et al*: Atorvastatin enhances the therapeutic efficacy of mesenchymal stem cells-derived exosomes in acute myocardial infarction via up-regulating long non-coding RNA H19. Cardiovasc Res 116: 353-367, 2020.
22. Yue Y, Li YQ, Fu S, Wu YT, Zhu L, Hua L, Lv JY, Li YL and Yang DL: Osthole inhibits cell proliferation by regulating the TGF-β1/Smad/p38 signaling pathways in pulmonary arterial smooth muscle cells. Biomed Pharmacother 121: 109640, 2020.
23. Charles Richard JL and Eichhorn PJA: Platforms for investigating lncRNA functions. SLAS Technol 23: 493-506, 2018.
24. Tan J, Liu S, Jiang Q, Yu T and Huang K: lncRNA-MIAT increased in patients with coronary atherosclerotic heart disease. Cardiol Res Pract 2019: 6280194, 2019.
25. Liao J, Wang J, Liu Y, Li J and Duan L: Transcriptome sequencing of lncRNA, miRNA, mRNA and interaction network constructing in coronary heart disease. BMC Med Genomics 12: 124, 2019.
26. Lin XL, Hu HJ, Liu YB, Hu XM, Fan XJ, Zou WW, Pan YQ, Zhou WQ, Peng MW and Gu CH: Allicin induces the upregulation of ABCA1 expression via PPARγ/LXRα signaling in THP-1 macrophage-derived foam cells. Int J Mol Med 39: 1452-1460, 2017.
27. Livak KJ and Schmittgen TD: Analysis of relative gene expression data using real-time quantitative PCR and the 2(-Delta Delta C(T)) method. Methods 25: 402-408, 2001.
28. Cui Y, Fu S, Sun D, Xing J, Hou T and Wu X: EPC-derived exosomes promote osteoclastogenesis through lncRNA-MALAT1. J Cell Mol Med 23: 3843-3854, 2019.
29. National Research Council Committee for the Update of the Guide for the Care and Use of Laboratory Animals: The National Academies Collection: Reports funded by National Institutes of Health. In: Guide for the Care and Use of Laboratory Animals. 8th edition. National Academies Press, Washington, DC, 2011.
30. Shen S, Zheng X, Zhu Z, Zhao S, Zhou Q, Song Z, Wang G and Wang Z: Silencing of GAS5 represses the malignant progression of atherosclerosis through upregulation of miR-135a. Biomed Pharmacother 118: 109302, 2019.
31. Guo Z, Zhao Z, Yang C and Song C: Transfer of microRNA-221 from mesenchymal stem cell-derived extracellular vesicles inhibits atherosclerotic plaque formation. Transl Res 226: 83-95, 2020.
32. Yu XH, Zhang DW, Zheng XL and Tang CK: Cholesterol transport system: An integrated cholesterol transport model involved in atherosclerosis. Prog Lipid Res 73: 65-91, 2019.
33. Ertek S: High-density lipoprotein (HDL) dysfunction and the future of HDL. Curr Vasc Pharmacol 16: 490-498, 2018.
34. Kennedy MA, Barrera GC, Nakamura K, Baldán A, Tarr P, Fishbein MC, Frank J, Francone OL and Edwards PA: ABCG1 has a critical role in mediating cholesterol efflux to HDL and preventing cellular lipid accumulation. Cell Metab 1: 121-131, 2005.
35. Talbot CPJ, Plat J, Ritsch A and Mensink RP: Determinants of cholesterol efflux capacity in humans. Prog Lipid Res 69: 21-32, 2018.
36. Wang H, Yang Y, Sun X, Tian F, Guo S, Wang W, Tian Z, Jin H, Zhang Z and Tian Y: Sonodynamic therapy-induced foam cells apoptosis activates the phagocytic PPARγ-LXRα-ABCA1/ABCG1 pathway and promotes cholesterol efflux in advanced plaque. Theranostics 8: 4969-4984, 2018.
37. Mao MJ, Hu JP, Wang C, Zhang YY and Liu P: Effects of Chinese herbal medicine Guanxinkang on expression of PPARγ-LXRα-ABCA1 pathway in ApoE-knockout mice with atherosclerosis. Zhong Xi Yi Jie He Xue Bao 10: 814-820, 2012 (In Chinese).
38. Li Y, Shi G, Han Y, Shang H, Li H, Liang W, Zhao W, Bai L and Qin C: Therapeutic potential of human umbilical cord mesenchymal stem cells on aortic atherosclerotic plaque in a high-fat diet rabbit model. Stem Cell Res Ther 12: 407, 2021.
39. Kirwin T, Gomes A, Amin R, Sufi A, Goswami S and Wang B: Mechanisms underlying the therapeutic potential of mesenchymal stem cells in atherosclerosis. Regen Med 16: 669-682, 2021.
40. Hashem RM, Rashed LA, Abdelkader RM and Hashem KS: Stem cell therapy targets the neointimal smooth muscle cells in experimentally induced atherosclerosis: Involvement of intracellular adhesion molecule (ICAM) and vascular cell adhesion molecule (VCAM). Braz J Med Biol Res 54: e10807, 2021.
41. Zhang X, Huang F, Li W, Dang JL, Yuan J, Wang J, Zeng DL, Sun CX, Liu YY, Ao Q, *et al*: Human gingiva-derived mesenchymal stem cells modulate monocytes/macrophages and alleviate atherosclerosis. Front Immunol 9: 878, 2018.
42. Chen S, Zhou H, Zhang B and Hu Q: Exosomal miR-512-3p derived from mesenchymal stem cells inhibits oxidized low-density lipoprotein-induced vascular endothelial cells dysfunction via regulating Keap1. J Biochem Mol Toxicol 35: 1-11, 2021.
43. Yang Y, Ye Y, Su X, He J, Bai W and He X: MSCs-derived exosomes and neuroinflammation, neurogenesis and therapy of traumatic brain injury. Front Cell Neurosci 11: 55, 2017.
44. Yu C, Tang W, Lu R, Tao Y, Ren T and Gao Y: Human adipose-derived mesenchymal stem cells promote lymphocyte apoptosis and alleviate atherosclerosis via miR-125b-1-3p/BCL11B signal axis. Ann Palliat Med 10: 2123-2133, 2021.
45. Wang H, Gong H, Liu Y and Feng L: Relationship between lncRNA-Ang362 and prognosis of patients with coronary heart disease after percutaneous coronary intervention. Biosci Rep 40: BSR20201524, 2020.
46. Mao Q, Liang XL, Zhang CL, Pang YH and Lu YX: lncRNA KLF3-AS1 in human mesenchymal stem cell-derived exosomes ameliorates pyroptosis of cardiomyocytes and myocardial infarction through miR-138-5p/Sirt1 axis. Stem Cell Res Ther 10: 393, 2019.
47. Li H, Han S, Sun Q, Yao Y, Li S, Yuan C, Zhang B, Jing B, Wu J, Song Y and Wang H: Long non-coding RNA CDKN2B-AS1 reduces inflammatory response and promotes cholesterol efflux in atherosclerosis by inhibiting ADAM10 expression. Aging (Albany NY) 11: 1695-1715, 2019.
48. Meng XD, Yao HH, Wang LM, Yu M, Shi S, Yuan ZX and Liu J: Knockdown of GAS5 inhibits atherosclerosis progression via reducing EZH2-mediated ABCA1 transcription in $ApoE^{-/-}$ mice. Mol Ther Nucleic Acids 19: 84-96, 2020.

49. Zhang ZZ, Chen JJ, Deng WY, Yu XH and Tan WH: CTRP1 decreases ABCA1 expression and promotes lipid accumulation through the miR-424-5p/FoxO1 pathway in THP-1 macrophage-derived foam cells. Cell Biol Int, Jul 20, 2021 (Epub ahead of print). doi: https://doi.org/10.1002/cbin.11666.
50. Moradi-Chaleshtori M, Shojaei S, Mohammadi-Yeganeh S and Hashemi SM: Transfer of miRNA in tumor-derived exosomes suppresses breast tumor cell invasion and migration by inducing M1 polarization in macrophages. Life Sci 282: 119800, 2021.
51. Zhao R, Feng J and He G: miR-613 regulates cholesterol efflux by targeting LXRα and ABCA1 in PPARγ activated THP-1 macrophages. Biochem Biophys Res Commun 448: 329-334, 2014.
52. Xu Y, Lai F, Xu Y, Wu Y, Liu Q, Li N, Wei Y, Feng T, Zheng Z, Jiang W, *et al*: Mycophenolic acid induces ATP-binding cassette transporter A1 (ABCA1) expression through the PPARγ-LXRα-ABCA1 pathway. Biochem Biophys Res Commun 414: 779-782, 2011.
53. Gu HF, Li N, Xu ZQ, Hu L, Li H, Zhang RJ, Chen RM, Zheng XL, Tang YL and Liao DF: Chronic unpredictable mild stress promotes atherosclerosis via HMGB1/TLR4-mediated downregulation of PPARγ/LXRα/ABCA1 in ApoE$^{-/-}$ mice. Front Physiol 10: 165, 2019.
54. Wang S, Zhang X, Liu M, Luan H, Ji Y, Guo P and Wu C: Chrysin inhibits foam cell formation through promoting cholesterol efflux from RAW264.7 macrophages. Pharm Biol 53: 1481-1487, 2015.

This work is licensed under a Creative Commons Attribution-NonCommercial-NoDerivatives 4.0 International (CC BY-NC-ND 4.0) License.